994 *J. Am. Chem. Soc.* **2000,** *122,* 994−995

# Monolithic Mesoporous Silica Templated by Microemulsion Liquid Crystals

Pingyun Feng,[†] Xianhui Bu,[‡] Galen D. Stucky,*[,‡] and
David J. Pine*[,†]

*Department of Chemical Engineering and*
*Department of Chemistry, University of California*
*Santa Barbara, California 93106*

*Received August 12, 1999*

Despite success in the synthesis of mesoporous materials in various meso- and macroscopic forms,[1−11] the simultaneous control of pore size and morphology in monolithic structures has been hampered by the lack of a generalized synthetic method suitable to multicomponent systems such as microemulsion multiphase compositions. Known procedures for the preparation of thin films, fibers, spheres, or monoliths of mesoporous silica include solvent evaporation in nonaqueous (e.g., ethanol) systems and growth of fibers and thin films at interfaces.[12,13] The pore size of mesophases obtained from these procedures is in general limited by surfactant lengths and the restricted range of compositions. Organic species such as 1,3,5-trimethylbenzene (TMB) that were reported to be useful in the pore size expansion of powdery forms[14,15] of mesoporous silica have been ineffective in controlling the pore size of monolithic silica mesophases.

Direct templating by liquid crystal phases has been recognized as a method for controlling morphology and preparing large monolithic mesophases,[16,17] but the method used so far is in general restricted to only a few surfactant/water binary systems.[17] While the pore size can be varied in some cases, the long-range ordering is usually lost.[18,19] Here we report a generalized method for the synthesis of periodic mesoporous silica by direct liquid crystal templating in multicomponent surfactant and cosurfactant systems. This method extends direct liquid crystal templating to more complex ternary (surfactant/cosurfactant/water) and microemulsion-type quaternary (surfactant/cosurfactant/water/oil) systems and thus leads to a greatly enhanced control over surfactant phase domains, mesoporous structural diversity, and macroscale morphology.

Our multicomponent systems consist of (1) surfactants such as Pluronic F127 and P123,[20] (2) cosurfactants such as butanol, pentanol, and hexanol, (3) aqueous silica sol, and (4) optionally oils such as octane. Both cosurfactants and oils are commonly used in the formulation of microemulsions. Microemulsion mesophases with long-range ordering were demonstrated by Tabony in 1986.[21] More recently, microemulsion droplets were proposed to be templates for the formation of mesocellular siliceous foams (MCFs).[15]

In a typical synthesis, the colloidal silica was prepared by mixing an aqueous dilute HCl solution (pH ≈ 2) with tetramethoxysilane (TMOS) and added to a mixture of Pluronic F127 and butanol. The methanol from the hydrolysis of TMOS was removed under vacuum. For a typical synthesis in a ternary system, the initial mass ratio was F127 (1.00):butanol (0.428): $H_2O$/HCl (1.58):TMOS (2.29). For a typical preparation in a microemulsion type quaternary system, the initial mass ratio was F127 (1.00):butanol (0.828):$H_2O$/HCl (1.91):octane (0.695): TMOS (3.14). The birefringent hexagonal liquid crystal phases are formed immediately upon complete mixing of these ingredients, whereas the polymerization and gelation of silica precursors usually take longer (e.g., a few hours). Liquid crystal phases, once formed, are preserved throughout the synthetic process and directly control the architecture of inorganic mesophases.

The inorganic polymerization process is monitored by the viscosity of liquid crystals, polarizing optical microscopy, and small-angle X-ray diffraction. The optically transparent monolithic gel takes the shape of the reaction vessel (Figure 1). Mesoporous silica materials are obtained by calcination at 450 °C for 6 h or by repeated extraction with ethanol at 60 °C. The XRD patterns confirm the immediate formation of mesophases when the colloidal silica and a cosurfactant such as butanol are added to the surfactant (Figure 2). Depending on component concentrations, the *d* spacing of the (100) peak for initial liquid crystals ranges from 105 to 189 Å, and the corresponding *d* spacing of calcined samples ranges from 73 to 168 Å for ordered hexagonal phases. Samples with even larger *d* spacing and uniform pore sizes have been obtained, but their periodic ordering has not been confirmed. During the gelation, aging, and calcination steps, a significant decrease in the *d* spacing of the (100) peak is observed (Figure 2). However, the long-range ordering is preserved throughout the shrinkage process. The large shrinkage in the *d* spacing can be greatly reduced by the hydrothermal treatment of the gelled sample at 100 °C for 24 h prior to calcination (Figure 2) or by using ethanol extraction to remove the organic species.

In addition to Pluronic F127, our method is applicable to other surfactants such as P123. For example, hexagonal silica mesophases have been prepared using Pluronic P123 in the ternary system (Figure 3). Both as-synthesized and calcined samples exhibit a minimum of three diffraction peaks. The pore size can be further tuned by using different cosurfactants or using microemulsion compositions involving both cosurfactants and oils. For example, the addition of octane into the F127/butanol/water system increases the *d* spacing of the (100) peak from 113 to 158 Å (the BdB−FHH[22] pore size from 77 to 116 Å) for the calcined hexagonal mesophase (Figure 3), whereas the substitution of butanol by pentanol gives an increase in *d* spacing of the (100) peak from 113 to 128 Å (the BdB−FHH pore sizes from 77 to 92 Å) for the calcined samples with the hexagonal structure

---

[†] Department of Chemical Engineering.

[‡] Department of Chemistry.

(1) Kim, S. S.; Zhang, W.; Pinnavaia, T. J. *Science* **1998**, *282*, 1302−1305.

(2) Kresge, C. T.; Leonowicz, M. E.; Roth, W. J.; Vartuli, J. C.; Beck, J. S. *Nature* **1992**, *359*, 710−712.

(3) Johnson, S. A.; Ollivier, P. J.; Mallouk, T. M. *Science* **1999**, *283*, 963−965.

(4) Vartuli, J. C.; Schmitt, K. D.; Kresge, C. T.; Roth, W. J.; Leonowicz, M. E.; McCullen, S. B.; Hellring, S. D.; Beck, J. S.; Schlenker, J. L.; Olson, D. H.; Sheppard, E. W. *Chem. Mater*. **1994**, *6*, 2317−2326.

(5) Yang, H.; Coombs, N.; Ozin, G. A. *Nature* **1997**, *386*, 692−695.

(6) Braun, P. V.; Osenar, P.; Stupp, S. I. *Nature* **1996**, *380*, 325−328.

(7) Tolbert, S. H.; Firouzi, A.; Stucky, G. D.; Chmelka, B. F. *Science* **1997**, *278*, 264−268.

(8) Kriesel, J. W.; Tilley, T. D. *Chem. Mater*. **1999**, *11*, 1190−1193.

(9) Gimon-Kinsel, M. E.; Balkus, K. J. *Microporous Mesoporous Mater*. **1999**, *28*, 113−123.

(10) Moller, K.; Bein, T. *Chem. Mater*. **1998**, *10*, 2950−2963

(11) Schacht, S.; Huo, Q.; Voigt-Martin, I. G.; Stucky, G. D.; Schuth, F. *Science* **1996**, *273*, 768−771.

(12) Melosh, N. A.; Lipic, P.; Bates, F. S.; Wudl, F.; Stucky, G. D.; Fredrickson, G. H.; Chmelka, B. F. *Macromolecules* **1999**, *32*, 4332−4342.

(13) Lu, Y.; Ganguli, R.; Drewien, C. A.; Anderson, M. T.; Brinker, C. J.; Gong, W.; Guo, Y.; Soyez, H.; Dunn, B.; Huang, M. H.; Zink, J. I. *Nature* **1997**, *389*, 364−368.

(14) Zhao, D.; Feng, J.; Huo, Q.; Melosh, N.; Fredrickson, G. H.; Chmelka, B. F.; Stucky, G. D. *Science* **1998**, *279*, 548−552.

(15) Schmidt-Winkel, P.; Lukens, W. W., Jr.; Zhao, D.; Yang, P.; Chmelka, B. F.; Stucky, G. D. *J. Am. Chem. Soc*. **1999**, *121*, 254−255.

(16) Goltner, C. G.; Henke, S.; Weissenberger, M. C.; Antonietti, M. *Angew. Chem., Int. Ed.* **1998**, *37*, 613−616.

(17) Attard, G. S.; Glyde, J. C.; Goltner, C. G. *Nature* **1995**, *378*, 366−368.

(18) Goltner, C. G.; Berton, B.; Kramer, E.; Antonietti, M. *Adv. Mater*. **1999**, *11*, 395−398.

(19) McGrath, K. M.; Dabbs, D. M.; Yao, N.; Aksay, I. A.; Gruner, S. M. *Science* **1997**, *277*, 552−556.

(20) The chemical formulas are $EO_{106}PO_{70}EO_{106}$ for F127 and $EO_{20}PO_{70}EO_{20}$ for P123, where EO = $-CH_2CH_2O-$ and PO = $-CH_2(CH_3)CHO-$.

(21) Tabony, J. *Nature* **1986**, *320*, 338−340.

(22) Lukens, W. W., Jr.; Schmidt-Winkel, P.; Zhao, D.; Feng, J.; Stucky, G. D. *Langmuir* **1999**, *15*, 5403−5409.

10.1021/ja992921j CCC: $19.00

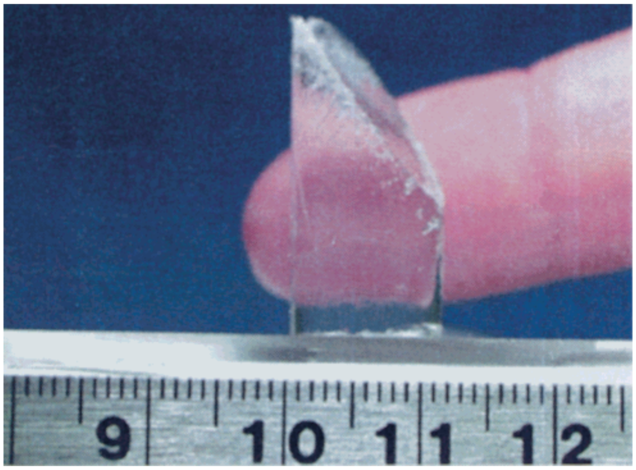

**Figure 1.** Monolithic surfactant−silica mesophase prepared using F127 as surfactant and butanol as cosurfactant. Upon surfactant removal by ethanol extraction and critical point drying, cracks are observed.

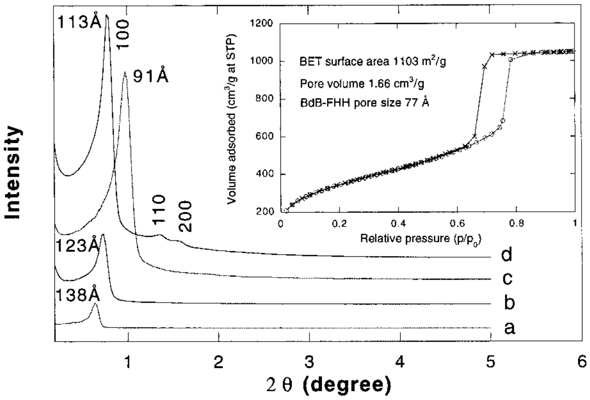

**Figure 2.** XRD patterns of as-synthesized and calcined hexagonal mesophases prepared from the F127/butanol/water system: (a) freshly prepared liquid crystal phase with colloidal silica in the aqueous domain; (b) after gelation; (c) after calcination; (d) hydrothermally treated at 100 °C for 24 h and then calcined. XRD patterns were recorded on a Scintag PAD X diffractometer using Cu Kα radiation. Inset: Nitrogen adsorption (○)−desorption (×) isotherm for sample d, Nitrogen sorption was done on a Micromeritics ASAP 2000 system at 77 K with samples degassed at 180 °C under vacuum for at least 6 h.

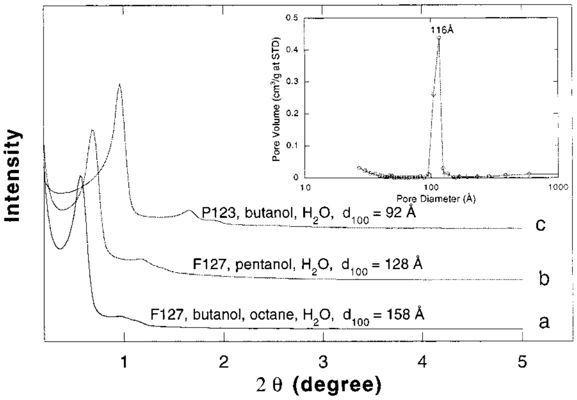

**Figure 3.** XRD patterns of calcined hexagonal mesophases showing the pore size control in multicomponent systems. Inset: The BdB−FHH pore size distribution curve from the desorption branch for sample a.

(Figure 3). By changing types or concentrations of surfactant, cosurfactant, or oil, silica monoliths with a range of pore sizes have been obtained. These mesoporous materials have high thermal and hydrothermal stabilities, and their mesoscopic ordering is retained even after heating in air at 800 °C for several hours or in boiling water for a few days.

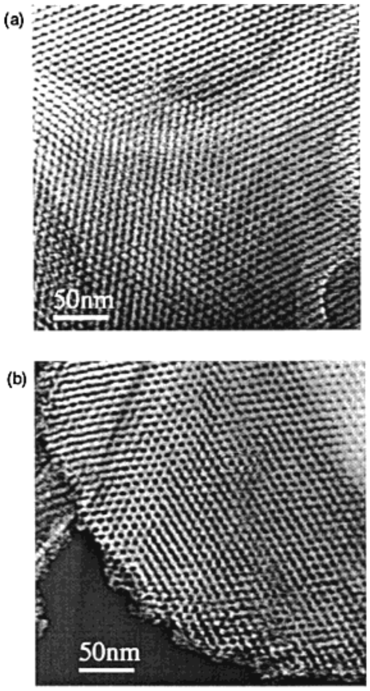

**Figure 4.** (a) Transmission electron micrograph of sample c in Figure 2. The BdB−FHH pore size determined from the desorption branch of the isotherm curve is 47 Å. (b) Transmission electron micrograph of sample d in Figure 2 before calcination, but after hydrothermal treatment. Transmission electron microscopy was performed on a JEOL 2000FX microscope (200 kV) using copper grids.

The periodic mesoporous structures have been confirmed by transmission electron microscopy images of both as-synthesized (with and without hydrothermal treatment) and calcined samples, showing highly ordered hexagonal arrays of mesopores (Figure 4) or equidistant parallel lines related to the hexagonal repeat between tubules. Consistent with the presence of uniform mesopores, the nitrogen adsorption−desorption isotherms show the expected type IV adsorption isotherm behavior with a type H1 hysteresis loop (Figure 2) with BET surface areas ranging from 419 to 1103 $m^2/g$ and the BdB−FHH pore sizes extending from 45 to 116 Å for the hexagonal phase.

In conclusion, this synthetic method is well suited for direct liquid crystal templating in ternary and microemulsion-type quaternary systems while preserving long-range ordering at the mesoscopic level. The advantage of this method is the feasibility of fabricating large monoliths of periodic mesoporous materials in combination with a high degree of control over the phase structure and pore size. The use of a range of cosurfactants adds a new dimension to the art of designed synthesis of porous materials. The success of templating by liquid crystals formed from quaternary microemulsion composition opens a new phase space in the synthesis and applications of meso- and macroporous materials.

**Acknowledgment.** This work was supported by the U.S. Army Research Office under Grant DAAG55-97-1-0372 (D.P.) and by the National Science Foundation under Grant CTS 98-71970 (D.P.). We thank Peidong Yang for help with TEM and Vinothan N. Manoharan for help with imaging monoliths. This work made use of Materials Research Laboratory Central Facilities supported by NSF under award DMR-9632716.

**Supporting Information Available:** Figures of X-ray powder diffraction pattern, nitrogen adsorption−desorption isotherm, pore size distribution, and TEM (PDF). This material is available free of charge via the Internet at http://pubs.acs.org.

JA992921J